J. Min. Metall. Sect. B-Metall. 53 (3) B (2017) 285 - 293

Journal of Mining and Metallurgy, Section B: Metallurgy

WETTING BEHAVIOR AND REACTIVITY BETWEEN LIQUID Gd AND ZrO_2 SUBSTRATE

P. Turalska [a, *], M. Homa [a], G. Bruzda [a], N. Sobczak [a, b], I. Kaban [c], N. Mattern [c], J. Eckert [d, e]

[a] Foundry Research Institute, Krakow, Poland
[b] Institute of Precision Mechanics, Warsaw, Poland
[c] IFW Dresden, Institute for Complex Materials, Dresden, Germany
[d] Erich Schmidt Institute of Materials Science, Austrian Academy of Sciences, Leoben, Austria
[e] Department Materials Physics, Montanuniversität Leoben, Leoben, Austria

(Received 15 August 2017; accepted 04 October 2017)

Abstract

The wetting behavior and reactivity between molten pure Gd and polycrystalline 3YSZ substrate (ZrO_2 stabilized with 3 wt% of Y_2O_3) were experimentally determined by a sessile drop method using a classical contact heating coupled with drop pushing procedure. The test was performed under an inert flowing gas atmosphere (Ar) at two temperatures of 1362 °C and 1412 °C. Immediately after melting (T_m=1341 °C), liquid Gd did not wet the substrate forming a contact angle of θ=*141*°. The non-wetting to wetting transition ($\theta < 90°$) took place after about 110 seconds of interaction and was accompanied by a sudden decrease in the contact angle value to *67*°. Further heating of the couple to 1412 °C did not affect wetting (θ=*67°±1°)*.

The solidified Gd/3YSZ couple was studied by means of optical microscopy and scanning electron microscopy coupled with X-ray energy dispersive spectroscopy. Structural investigations revealed that the wettability in the Gd/3YSZ system is of a reactive nature associated with the formation of a continuous layer of a wettable reaction product $Gd_2Zr_2O_7$.

Keywords: Gd; ZrO_2; Sessile drop; Wettability; Reactivity; Interfaces.

1. Introduction

Gadolinium (Gd) is widely used as alloying addition in advanced alloys to improve their functional and utility properties [1-5]. Many Gd-rich alloys exhibit a liquid–liquid miscibility gap thus making them also suitable for fabrication of microphase-separated metal matrix composites by the liquid-phase rout [6-10]. However, high melting temperature, high oxygen affinity and chemical aggressiveness against most available commercial refractories render and casting, as well as high-temperature testing of Gd-containing alloys using container-assisted [11-13] or substrate-assisted [14] methods (e.g. calorimetric studies, measurements of surface tension of liquid alloys) difficult.

Kaban et al. [14] adopted a sessile drop method for estimating the critical temperatures of Gd-Ti alloys placed on a ceramic substrate. The high temperature behavior of $Gd_{40}Ti_{60}$ and $Gd_{60}Ti_{40}$ alloys on the dense polycrystalline yttria Y_2O_3 and two kinds of yttria-stabilized zirconia (YSZ) substrates containing 3 wt% and 5 wt% of Y_2O_3 (3YSZ and 5YSZ, respectively) was studied in situ using high speed high resolution digital camera. It was observed that the Gd-rich liquid phase of both alloys wets Y_2O_3 (the contact angle q<90°) at a temperature of ~ 1350 °C, while during the next heating up to 1450 °C, the liquid formed is completely consumed due to liquid metal penetration inside the substrate. Therefore, Y_2O_3 was rejected as a candidate refractory for measurements of thermophysical properties of Gd-Ti alloys by substrate- or container-assisted techniques [14].

Similar tests performed with yttria-stabilized zirconia showed that the Gd-Ti melt reacts relatively strongly with 5YSZ. However, a reduction of the yttria content down to 3% in 3YSZ makes it more stable against Gd-Ti melts over a wide temperature range up to ~1650 °C. It was suggested that the thin reaction product layer formed at the interface contained gadolinium, zirconium and oxygen (designated as a GdZrO phase) preventing the

Dedicated to the memory of Professor Dragana Živković

* *Corresponding author: patrycja.turalska@iod.krakow.pl*

DOI:10.2298/JMMB170815045T

interdiffusion of components and a further growth of the reaction zone [14].

Sobczak et al. [15] measured the contact angles formed by liquid pure Gd on the same substrates of polycrystalline yttria and 3YSZ using the same testing device and conditions. They found that at a temperature of 1360 °C, pure Gd wets both substrates but the contact angle on Y_2O_3 (33°) is two times smaller than that on 3YSZ (68°). Moreover, addition of Ti or Ti-Zr to Gd results in worsening of the wetting of Y_2O_3 with liquid $Gd_{60}Ti_{40}$ (the contact angle of 33° was measured at much higher temperature of 1473 °C) or non-wetting with liquid $Gd_{30}Ti_{70}$ (q=157° at 1500° C). A similar effect and a non-wetting behavior of Gd-Ti-Zr alloys were noted on 3YSZ, showing θ=104-94° at T=1650-1717 °C. It was suggested that the interaction of both pure Gd and Gd-rich alloys with 3YSZ substrates is controlled by the formation of $Gd_2Zr_2O_7$ continuous interfacial reaction product [15].

However, a mechanisms of the high temperature interaction in the Gd/ZrO_2 couple accompanied with the mass transport and formation of an interfacial phase was not sufficiently analyzed in works [14,15].

This paper focuses on detailed examination of the high temperature behavior and the reactivity of liquid Gd with polycrystalline yttria-stabilized zirconia (3YSZ), including melting of Gd sample, and their temperature dependent wetting upon heating, and solidification.

2. Experimental

2.1. Materials

For high temperature investigations, pure Gd of 99.99% purity (Sigma Aldrich) and polycrystalline ZrO_2 stabilized with 3 wt% of Y_2O_3 were used. The substrate was made of ZrO_2 and Y_2O_3 powders having 99.9 % purity by high pressure-high temperature synthesis. The 3YSZ substrate surface was polished to a roughness of $R_a \approx 120$ nm. In order to prevent substrate contamination, the polishing was carried out by using the same powders that were used for the synthesis step. The as-prepared substrate was then ultrasonically cleaned in isopropanol (C_3H_8O) for 5 minutes using the Polsonic SONIC-2 device. Directly before high temperature testing, the substrate was preheated in air at 1000 °C for 5 h.

2.2 Methods

The wetting behavior was examined using an experimental set up for investigations of high temperature phenomena described in details in [16]. The tests were carried out by means of the sessile drop (SD) method [12-13], using two different procedures during one experiment: 1) a classical contact heating (ch), and 2) a drop pushing (dp).

The wettability tests were performed under flowing inert gas (Ar, 99.9992%) at a pressure of 850-900 hPa, at two temperatures (1362 °C and 1412 °C), marked as stage I and stage II in Figure 1. Firstly, the metal/substrate couple was contact heated starting from room temperature up to 1362 °C (i.e. 50 °C above the melting point of Gd) at a rate of 13 °C/min, and then it was held at this temperature for 5 minutes (stage I). Subsequently, the Gd/YSZ couple was slowly heated at a rate of 6 °C/min to 1412 °C (i.e. 100 °C above the melting point of Gd) and it was again hold for 5 minutes (stage II).

After the wettability test at 1412 °C, the liquid drop was pushed and slightly moved along the surface of the substrate by means of an alumina pusher in order to reveal the drop/substrate interface formed. The Al_2O_3 pusher was previously preheated at 1000 °C for 1 h in air. After the drop pushing, the sample was cooled down to room temperature at a rate of 26 °C/min.

The high temperature behavior of the drop/substrate couple was recorded using a Mikrotron 1310 high resolution digital camera at a rate of 10 frames per second (fps) during melting of Gd and during the test (stages I and II - Fig.1). During isothermal heating and cooling to the solidification temperature the recording was carried out at a rate of 1 fps. The collected data were used for a computer-aided analysis by means of the ASTRA2 software developed by IENI-CNR, Genua, Italy [17,18] and served as input for the calculation of the contact angle

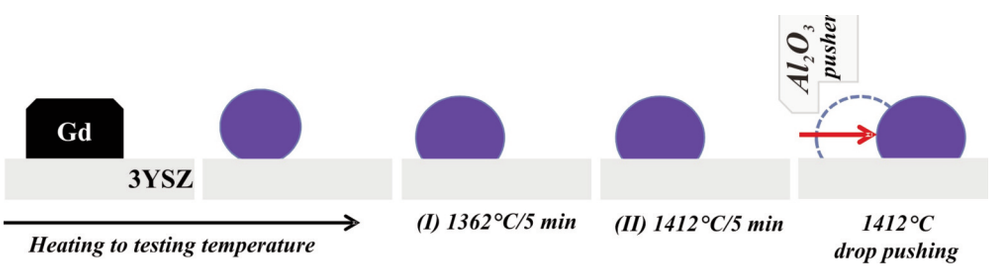

Figure 1. *Schematic illustration showing the sessile drop method (SD) coupled with contact heating (ch) procedure, including melting of the Gd sample during heating to the test temperature and testing at stages I and II, and the drop pushing (dp) procedure*

values θ (θ_l - left side angle; θ_r - right side angle and θ_{av} - average value of θ_l and θ_r), as well as for making a real-time movie of the high-temperature tests (SUPPLEMENT #1).

The microstructure and chemistry of the Gd/3YSZ couple after wettability test was examined with a Keyence VHX-700F optical microscope (OM) and Hitachi TM3000 scanning electron microscope (SEM) equipped with energy dispersive X-ray spectroscopy (EDS) analyser.

3. Results

Formation of a liquid Gd drop and its behavior on the 3YSZ substrate during melting and subsequent heating-holding at the stages I and II are represented by selected digital images in Figure 2 and in a real-time movie in SUPPLEMENT #1. The initially solid Gd sample (Fig. 2a) started to slightly change its shape at 1294 °C, i.e. after 101 minutes from the beginning of the heating process (Fig. 2b). With increasing temperature, the sample was gradually changing its shape. No discernible differences in the sample shape at 1306 °C (below the melting point) (Fig. 2c) and 1341 °C (above the melting point) (Fig. 2d) were noted.

Complete melting of the Gd sample was observed at 1341 °C, i.e. above the melting point of Gd (T_m=1312 °C) and was accompanied by a sudden decrease of the average contact angle value from θ_{av}=141° to θ_{av}=67° (Figs. 2d-e). Further heating to the test temperature of 1362 °C, holding for 5 minutes (Figs. 2f-g) and subsequent heating to the second stage temperature of 1412 °C and holding for 5 minutes (Figs. 2h-i) did not cause any further changes in the drop shape.

The kinetics of the contact angles measured between pure Gd and 3YSZ substrate are presented in Figure 3a. The analysis was initiated at the 102th minute of the experiment, when the metal started to melt. At the beginning (from 102th to 104th min), the kinetic curve showed a significant variation of the contact angle due to a non-homogeneous melting of the cuboid-like Gd sample that was gradually changing its shape. After reaching the melting temperature of Gd (1312 °C), the metal still did not form a typical drop shape and did not wet the substrate (θ>>90°). During further heating, a sudden decrease of the average contact angle value θ_{av} from 141° to 67°occured at 1341 °C, i.e. in the 104th min of interaction (Figs. 2d-e).

The contact angle fluctuations that occurred between the 104th and 108th minutes are presented at higher magnification in Figure 3b. A slight decrease in the contact angle value between the 104th and 105th minute was followed by a stabilization. Further heating of the system to the test temperature did not cause any changes in the wetting behavior and the final contact angle value remained θ_{av} =67°±1°.

After the wettability test at 1412 °C, an attempt was made to move the drop in order to reveal the drop/substrate interface at the test temperature directly in the chamber (Fig. 4). For this purpose, the alumina pusher, initially located above the drop, was moved down (Fig. 4a), touched the drop and slightly pushed it (Fig. 4b). During this short time manipulation it was noted that the drop wets the alumina pusher. Taking into account that the good wetting might be accompanied with a chemical reaction between the drop and Al_2O_3, only a slight displacement of the drop was done therefore. After that the alumina pusher was immediately detached from the drop (Fig. 4c).

Figures 5a-b depict the solidified Gd/3YSZ couple after high temperature testing. The initially white YSZ substrate became dark-gray due to a loss of oxygen [19] leading to the formation of nonstoichiometric ZrO_{2-x} upon heating. The Gd drop has a characteristic

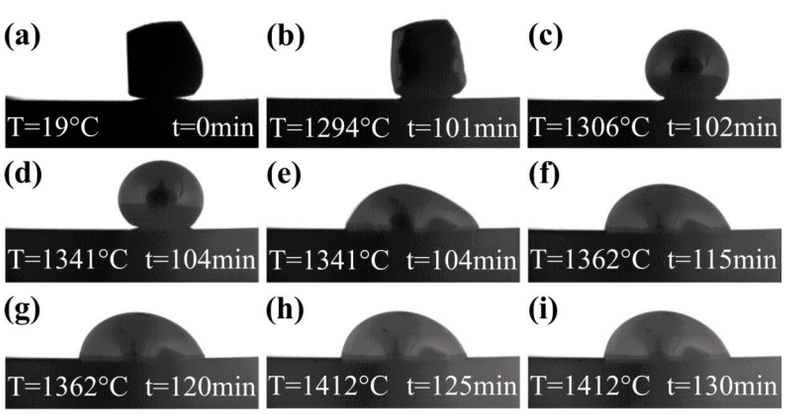

Figure 2. *Images recorded with a digital camera during the experiment: starting point (t=0) at the beginning of the experiment (a); heating to 1362°C showing the melting of the Gd sample (b-e) and changes in the drop shape (d, e); test at 1362°C (f-g); test at 1412°C (h-i)*

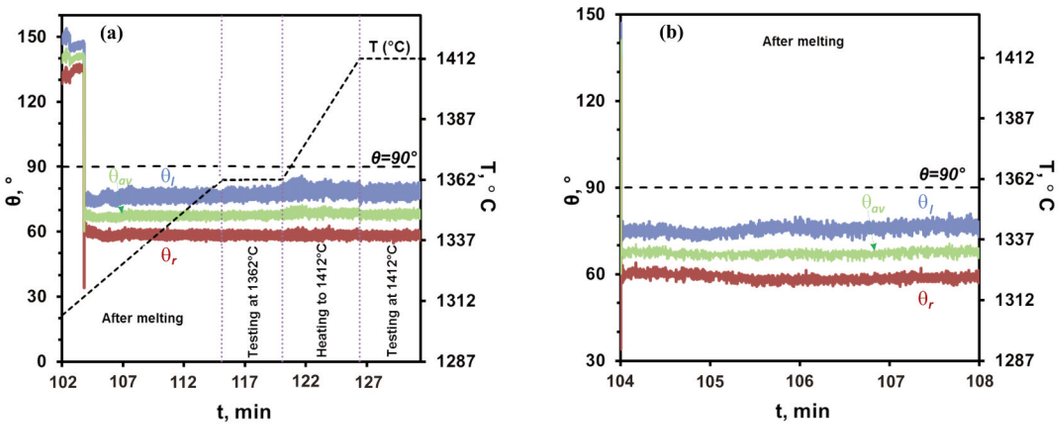

***Figure 3**. a) Wettability kinetics of the molten Gd on the 3YSZ substrate (SD/ch+dp); b) the contact angle fluctuations for the period of time between the 104th and 108th minutes*

non-symmetric shape coming from the attempt to push the drop to another position. The visual top-view observation of the couple shows that the drop surface is non-homogeneous and the areas with dissimilar colours are well distinguishable (grey, silver and gold). Moreover, the substrate surface has different grey shades showing an appearance of a ring around the drop, most probably caused from the evaporation and deposition of Gd on the substrate at the test temperature (Fig. 5b).

The SEM top-view observations and chemical analysis of the solidified couple (Figs. 6a-b) show a presence of different phases on the surface of initially pure Gd drop. The light grey irregular precipitates (Fig. 6a, P.1) and triangular precipitates (Fig. 6a, P.2) contain a high amount of gadolinium (up to 47.6 at.%) and oxygen (up to 56.0 at.%) as well as up to 4.1 at.% zirconium and up to 1.0 at.% yttrium. There are also dark grey irregular precipitates without yttrium (Fig. 6a, P. 4) on the surface of the drop. A big light grey area (Fig. 6a, P. 3) around the drop (from the side where the drop was pushed) corresponds to the exposed drop/substrate interface and represents a layer of reaction product, which was formed due to high temperature interaction in the Gd/3YSZ couple. The chemical analysis of the area around the drop (Fig. 5) revealed the presence of gadolinium on the substrate surface, which confirms the evaporation of

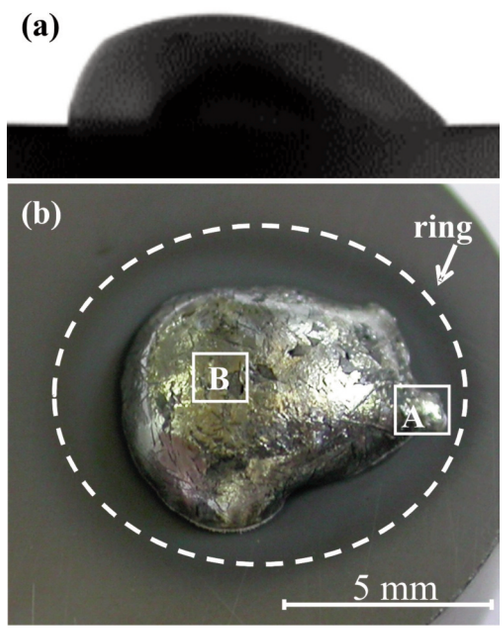

***Figure 5.** The Gd/3YSZ couple after the wettability test: a) the last image recorded by the digital camera after drop pushing at a temperature of 1412°C; b) top view of the solidified sessile drop couple: (A)area of the drop after the pushing attempt; (B) top of the drop*

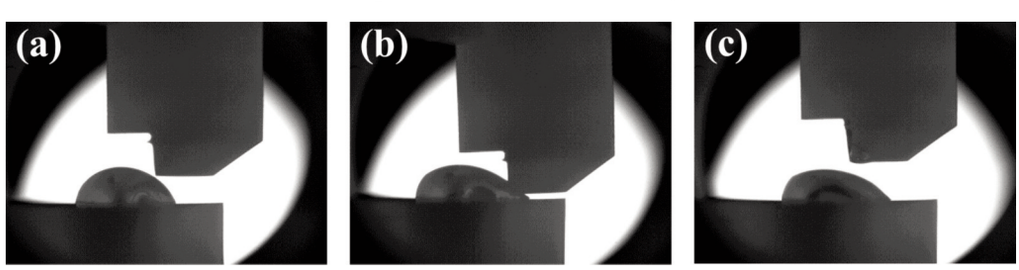

***Figure 4**. The drop pushing procedure at temperature of 1412°C; a) lowering of the Al_2O_3 pusher; b) drop pushing; c) rising of the Al_2O_3 pusher*

Gd and its deposition on the substrate during wettability test.

A detailed EDS analysis of the top of the drop (Fig. 6b) shows that the chemical composition of the light grey irregular precipitates (Fig. 6b, P.1-P.3) nearly matches the composition of very similar looking areas that are also visible at lower magnification (Fig. 6a, P.1). Using higher magnifications allowed determining the composition of the dark grey irregular precipitates (Fig. 6a, P.7-P.8), which are visible in Figure 6a as small, dark spots. They are yttrium-free but besides gadolinium and oxygen they contain also zirconium (up to 0.8 at. %). EDS analysis revealed that the matrix of the drop (Fig. 6a, P. 4-6) is mainly composed of gadolinium, but a small amount of zirconium was also identified (up to 2.3 at.%). The presence of zirconium and yttrium in the solidified drop indicates dissolution of the substrate in the liquid Gd.

The results of OM observations of the cross-sectioned couple are presented in Figure 7. Under a low magnification, long and irregular precipitates in the drop and a continuous reaction product layer (RPL) at the drop/substrate interface are observed (Figs. 7a-b). The RPL layer has the same color over its entire thicknesses and it grown beyond the drop area, which suggests that the wettability in the Gd/3YSZ system is of a reactive nature.

At higher magnification (Fig. 7c), the RPL layer is composed of two well-distinguished sublayers with different shades of grey. The light-grey, substrate-side sublayer #1 has a fine structure composed of regular shaped grains. The drop-side sublayer #2 is built of large and dark-grey crystals growing in the direction perpendicular to the substrate surface. Inside the drop, a white phase surrounding the grey phase is also visible (Fig. 7b). In addition, long needle-like dark grey precipitates are visible in the matrix of the drop (Fig. 7c) and they correspond to the dark needles shown in Fig. 7a.

The results of SEM/EDS analysis of the top of the drop are presented in Fig. 8a. Neither the dark grey participates (Fig. 8a, P.1-P.3) inside the drop nor those found on the surface (Fig. 8a, P.10) contain yttrium. Moreover, no yttrium was detected in the Gd-matrix (Fig. 8a, P.4-P.9). The dark grey precipitates are mostly composed of Gd (up to 57.4 at.%) and oxygen (up to 35.6 at.%), while the Gd-matrix contains a significantly lower content of oxygen (up to 7.4 at.%). Additionally, the results of EDS evaluations (Fig. 8a, P.10) allows recognizing these precipitates on the drop surface as Gd_2O_3 (most probably, residual surface oxide). A typical SEM image showing the drop structure in its central part is displayed in Figure 8b. The visible large and dark grey precipitates consist mainly of gadolinium and oxygen. They are similar to those observed at the top of the drop (Fig. 8a, P.1-P.3),

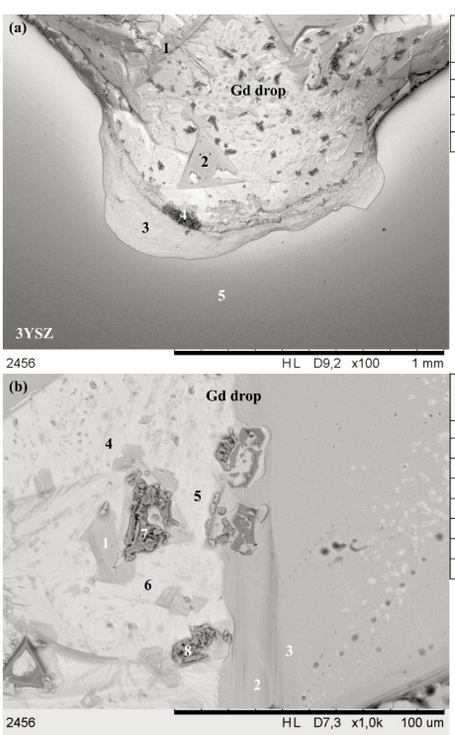

P.	Chemical composition, at.%			
	Gd	Zr	Y	O
1	40.5	2.5	1.0	56.0
2	47.6	4.1	0.3	48.0
3	36.5	4.1	0.0	59.4
4	42.2	5.9	0.3	51.6
5	11.3	25.1	2.1	61.5

P.	Chemical composition, at.%			
	Gd	Zr	Y	O
1	57.2	0.0	0.0	42.8
2	45.6	0.9	0.6	52.9
3	52.4	0.1	0.2	47.3
4	82.2	0.3	0.0	17.5
5	83.2	2.3	0.0	14.5
6	84.7	0.5	0.0	14.8
7	37.7	0.8	0.0	61.5
8	55.4	0.0	0.0	44.6

Figure 6. *SEM top-view image and EDS analysis of the drop surface after the wettability tests.: a) the (A) section (highlighted in Fig. 5); b) top-view SEM image of the drop (highlighted as the (B) section in Fig. 5)*

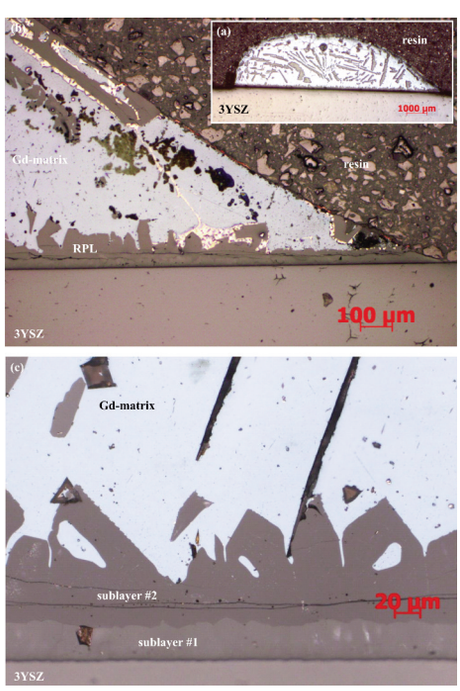

Figure 7. *Microstructure of a cross-sectioned sessile drop sample (OM): a) a panoramic view of the drop; b) right side of the drop; c) OM image showing the interface in the central part of the drop*

but their zirconium content (up to 0.4 at.%) is relatively lower and it is balanced by a higher content of oxygen. Moreover, in this part of the drop, a small content of yttrium (up to 0.6 at.%) was recorded both inside the precipitates and the Gd-matrix.

Figure 9a shows a detailed structure of the Gd drop from the substrate side with corresponding EDS analysis at the marked points. These results confirm the occurrence of a continuous layer made of two clearly distinguished sublayers with dissimilar structure, identified by OM (Fig. 7c). The sublayer #1 formed during interaction of Gd with the 3YSZ substrate is composed of gadolinium and oxygen with dissolved zirconium (up to 11.2 at.%) and yttrium (up to 1.9 at.%). The sublayer #2 contains large crystals grown into the Gd drop. This sublayer is mainly composed of gadolinium and oxygen, and it is enriched in zirconium (up to 7.5 at.%) and small amount of yttrium (up to 1.6 at.%). Furthermore, long dark grey precipitates in the form of needles were identified in the vicinity of the interface. They are composed of gadolinium and oxygen as well as dissolved zirconium and yttrium (Fig. 9a, P.6), while the matrix of the drop consists of a Gd-based solid solution of oxygen (up to 19.1 at.%), zirconium (up to 7.7 at.%), and yttrium (up to 2.4 at.%). The morphology and location of these precipitates at the interface suggest that they were formed rather during the cooling process, than as the direct effect of a reaction between the drop and the substrate. It should be emphasized that our results of EDS characterization of the interfacial layer formed in the Gd/ZrO_2 couple agree well with those obtained for the $Gd_2Zr_2O_7$ phase by Wang et al. [20] who also identified this phase by X-ray diffraction.

Figures 9b-c show the presence of a white phase, previously identified by means of OM. SEM/EDS investigations performed at a higher magnification revealed that this phase is composed of bright-grey areas and dark-grey participates. Chemical composition analysis of the bright areas revealed mainly Gd (up to 69.5 at.%). The content of Zr and O are 18.2 at.% and 15.2 at.%, respectively. On the other hand, the dark-grey precipitates have almost the same Zr content and significantly higher oxygen concentration (51.3 at.%).

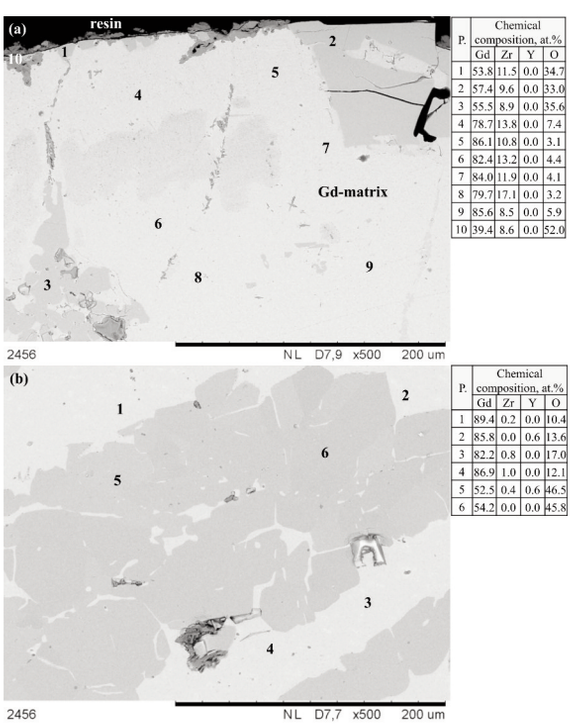

P.	Chemical composition, at.%			
	Gd	Zr	Y	O
1	53.8	11.5	0.0	34.7
2	57.4	9.6	0.0	33.0
3	55.5	8.9	0.0	35.6
4	78.7	13.8	0.0	7.4
5	86.1	10.8	0.0	3.1
6	82.4	13.2	0.0	4.4
7	84.0	11.9	0.0	4.1
8	79.7	17.1	0.0	3.2
9	85.6	8.5	0.0	5.9
10	39.4	8.6	0.0	52.0

P.	Chemical composition, at.%			
	Gd	Zr	Y	O
1	89.4	0.2	0.0	10.4
2	85.8	0.0	0.6	13.6
3	82.2	0.8	0.0	17.0
4	86.9	1.0	0.0	12.1
5	52.5	0.4	0.6	46.5
6	54.2	0.0	0.0	45.8

Figure 8. *SEM images of a cross-sectioned Gd/3YSZ couple with corresponding EDS analysis at the marked points: a) top of the drop; b) central part of the drop*

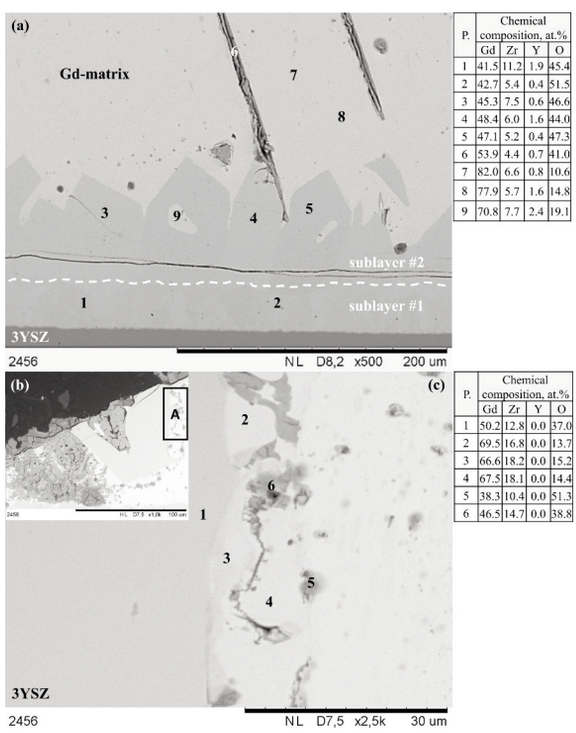

P.	Chemical composition, at.%			
	Gd	Zr	Y	O
1	41.5	11.2	1.9	45.4
2	42.7	5.4	0.4	51.5
3	45.3	7.5	0.6	46.6
4	48.4	6.0	1.6	44.0
5	47.1	5.2	0.4	47.3
6	53.9	4.4	0.7	41.0
7	82.0	6.6	0.8	10.6
8	77.9	5.7	1.6	14.8
9	70.8	7.7	2.4	19.1

P.	Chemical composition, at.%			
	Gd	Zr	Y	O
1	50.2	12.8	0.0	37.0
2	69.5	16.8	0.0	13.7
3	66.6	18.2	0.0	15.2
4	67.5	18.1	0.0	14.4
5	38.3	10.4	0.0	51.3
6	46.5	14.7	0.0	38.8

Figure 9. *SEM image of a cross-sectioned Gd/3YSZ couple with corresponding EDS analysis in the marked points: a) central part of the drop; b) thewhite phase visible in Fig. 7b (OM image) at low magnification; c) the white phase highlighted as the (A) section in Fig. 9a*

4. Discussion

The high temperature sessile drop tests performed at 1362 °C and 1412 °C show a good wetting between liquid Gd and the 3YSZ substrate forming a final contact angle with an average value $\theta_f = 67° \pm 1°$.

Structural characterization of the solidified

Gd/3YSZ couple did not show neither a crater nor a metal infiltrated zone in the substrate. However, SEM+EDS analysis points to dissolution of the substrate in liquid Gd and transport of both Zr and Y from the substrate into the drop, evidenced by the presence of these elements in the top of the drop. Furthermore, a continuous layer composed of Gd, Zr and O formed reactively at the interface. This layer is built of two sublayers with dissimilar structure and a well-distinguishable boundary between them (Fig. 7c). The similarity of the chemical compositions of these sublayers suggests that they present the same phase. The substrate-side sublayer with homogeneous thickness consist of fine grains (Fig. 7c). It has a light-grey colour in OM and contains more Gd, compared of the drop-side sublayer that is darker under optical microscope (Fig. 7c). Both the non-homogeneous thickness of the drop-side sublayer as well as the finding that is comprised of large crystals with well distinguishable growth direction perpendicular to the substrate surface suggest that this sublayer was formed during solidification while the substrate-side sublayer was formed by direct chemical reaction between the Gd drop and the 3YSZ substrate.

It is well established that a thermodynamic assessment of phase diagrams is a useful tool in materials research and process control, especially upon a development of new alloys [21].

Due to a lack of literature data for the Gd-Zr-O phase diagram, the interaction in the liquid Gd/ZrO_2 couple can be predicted using the reported data on the thermodynamic stability of oxides [22] and the experimentally evaluated binary phase diagrams Gd-Zr [23], Zr-O [24] and Gd_2O_3-ZrO_2 [25] as well as a tentative phase diagram calculated by McMurray for the Gd-O system using the CALPHAD method[26].

From the calculated data of [22], the standard free energy of formation ΔG° vs temperature has a negative value for both ZrO_2 and Gd_2O_3. Taking into account that at a testing temperature of 1412 °C, ΔG° of ZrO_2 is about -795 kJ/mol in contrast to about -920 kJ/mol for Gd_2O_3 one may conclude that the thermodynamic stability of ZrO_2 is lower than that of Gd_2O_3 and Gd may reduce zirconia according to the following redox reaction:

$$4Gd + 3ZrO_2 = 3Zr + 2Gd_2O_3 \quad (1)$$

The Gibbs energy of above mentioned reaction, calculated according to literature data [27], was equal to ΔG_r=-331 kJ/mol. However, structural characterization by SEM+EDS analysis in this study does not give a clear evidence for the formation of gadolinia in the Gd/ZrO_2 couple. On the other hand, large amounts of zirconium and oxygen in the solidified Gd drop are well documented. This is in good agreement with the literature data of the Gd-Zr phase diagram (Fig. 10a [23]) showing that liquid Gd may dissolve up to 30 at.% Zr under conditions of this study. Our SEM+EDS results are also in line with the predictions of McMurray [26] for the Gd-O phase diagram (Fig. 10b) since liquid Gd may dissolve up to 25 at.% oxygen at the maximum temperature of the sessile drop test (1412 °C). However, when the temperature reaches a value of 1160 °C during cooling, the Gd melt saturated with oxygen should decompose into the Gd-Gd_2O_3 eutectic containing a low-temperature modification of gadolinium oxide (C-phase in Fig. 10b). It is noteworthy that the formation of the Gd-Gd_2O_3 eutectic has not been observed in this work, nor has it been reported in any other experimental study. Moreover, the detailed examination of the cross-sectioned Gd/ZrO_2 couple did not reveal any crater in the substrate under the Gd drop as it is usually found in case of dissolutive wetting (see e.g. [28-31]). Furthermore, the analysis of the Gd_2O_3-ZrO_2 phase diagram [25] suggests that under the conditions of this study, the Gd_2O_3 phase is not stable in contact with the ZrO_2 substrate and the interaction at the Gd_2O_3/ZrO_2 interface should lead to the formation of ternary oxide (P - pyrochlore $Gd_2Zr_2O_7$ in Fig. 10c) by the following reaction:

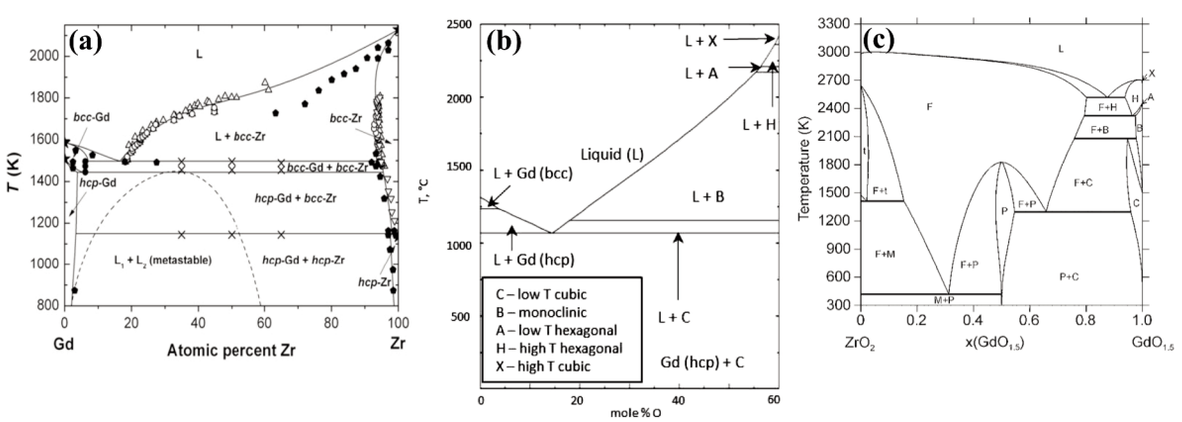

Figure 10. *Literature phase diagram data: a) Gd-Zr [23]; b) Gd-O [26]; c) Gd_2O_3-ZrO_2 [25]*

$$Gd_2O_3 + 2ZrO_2 = Gd_2Zr_2O_7 \quad (2)$$

The formation of $Gd_2Zr_2O_7$ by high temperature solid state reaction using Gd_2O_3 and ZrO_2 as raw materials has been confirmed experimentally at 1100–1600 °C under atmospheric pressure (e.g. [32]).

Thus the reaction between liquid Gd and zirconia can be summarized as follows:

$$4Gd + 7ZrO_2 = 3Zr + 2Gd_2Zr_2O_7 \quad (3)$$

Such a reaction was indeed observed at the Gd/ZrO_2 interface leading to the formation of a continuous and a dense layer of $Gd_2Zr_2O_7$ phase growing beyond the drop area (Fig. 7b). Therefore, it is believed that the good wetting of the zirconia substrate by liquid gadolinium observed in this study has a reactive nature while its mechanism is related to the formation of a wettable interfacial reaction product (pyrochlore $Gd_2Zr_2O_7$). For such kind of the reactive wetting systems, both the final degree of wetting as well as spreading are controlled by the new phase reactively formed at the metal/ceramic interface [33].

The formation of a continuous interfacial layer of $Gd_2Zr_2O_7$ phase may play a positive role in high temperature liquid-assisted processing or materials testing involving the contact of Gd-containing melts with YSZ ceramics. Its presence at the interface affects the kinetics of high temperature interaction between the melt and the refractory, thus making fast processing or testing without significant pollution of the melt with the refractory constituents possible.

5. Conclusions

Liquid gadolinium reacts and wets zirconia stabilized with 3% yttria forming a contact angle of 67° at both 1362 °C and 1412 °C. The good wetting in the Gd/3YSZ system is dominated by the formation of a continuous layer of the wettable reaction product $Gd_2Zr_2O_7$, growing at the drop/substrate interface as well as on the substrate surface beyond the drop.

The presence of the $Gd_2Zr_2O_7$ layer at the interface affects the kinetics of high temperature interaction between the melt and the refractory, thus making liquid-assisted processing or materials testing involving the contact of Gd-containing melts with YSZ ceramics without significant pollution of the melt with the refractory constituents possible.

Acknowledgements

This study was done in the frame of the collaboration program between the German Academic Exchange Service DAAD and the Ministry of Science and Higher Education of Poland. Financial supports from the National Science Centre of Poland (program HARMONIA, project No. 193624) and the German Academic Exchange Service DAAD (Project No. DAAD-56269397) are acknowledged. The authors acknowledge Dr. Rafał Nowak for technical assistance in scanning electron microscopy characterization.

References

[1] K.U. Kainer, Magnesium alloys and technologies, WILEY-VCH Verlag GmbH & Co. KG, Weinheim, 2003.

[2] Y. Hiramitsu, T. Homma and S. Kamado, Mater. Sci. Eng., 21 (2011) 1–8.

[3] L. Tissot and A. Blaise, J. Appl. Phys., (1970) 41(3) 1180–1182.

[4] J.H. Hsu and Y.W. Fu, J. Appl. Phys., 75(10) (1994) 7152–7154.

[5] V. Sidorov, P. Sveč, P. Sveč Sr., D. Janikovič, V. Mikhailov, E. Sidorova and L. Son, J. Magn. Mater., 408 (2016) 35–40.

[6] C. Wu, D. Ding, L. Xia, and K. C. Chan, AIP Adv., 6(3) (2016) 035302-1–035302-6.

[7] B. Schwarz, N. Mattern, Q. Luo and J. Eckert, J. Magn. Mater., 324 (2012) 1581–1587.

[8] I. Kaban, M. Köhler, L. Ratke, R. Nowak, N. Sobczak, N. Mattern, J. Eckert, A. L. Greer, S. W. Sohn and D. H. Kim, J. Mater. Sci., 47 (2012) 8360–8366.

[9] L. Zhang, M. Bao, Q. Zheng, L. Tian, and J. Du, AIP Adv., 6(3) (2016) 0353220.

[10] J.H. Han, N. Mattern, I. Kaban, D. Holland-Moritz, J. Bednarcik, R. Nowak, N. Sobczak, D. H. Kim and J. Eckert, J. Phys. Condens. Matter., 25 (2013) 245104-245111.

[11] G. Balducci, A. Ciccioli, G. de Maria, F. Hoda, and G. M. Rosenblatt, Pure Appl. Chem., 81(2) (2009) 299–338.

[12] N. Sobczak, J. Sobczak, R. Asthana, R. Purgert, China Foundry, 7(4) (2010) 425–437.

[13] N. Sobczak, M. Singh and R. Asthana, Curr. Opin. Solid State Mater. Sci., 9(4) (2005) 241–253.

[14] I. Kaban, R. Nowak, O. Shuleshova, B. Korpala, G. Bruzda, A. Siewiorek, J.H. Han, N. Sobczak and N. Mattern, J. Eckert, J .Mater. Sci., 47, (2012) 8381–8386.

[15] N. Sobczak, P. Turalska, M. Homa, A. Siewiorek, G. Bruzda, R. Nowak, A. Kudyba, I. Kaban, N. Mattern and J. Eckert, High temperature interaction between liquid Gd-containing alloys and selected oxides, Proc. of the 72nd World Foundry Congress, Nagoya, Japan, (2016).

[16] N. Sobczak, R. Nowak, W. Radziwill, J. Budzioch, and A. Glenz, Experimental complex for investigations of high temperature capillarity phenomena, Mater. Sci. Eng., (2008), A 495, p 43–49.

[17] L. Liggieri and A. Passerone, High Temp. Technol., 7(2) (1989) 82–86.

[18] ASTRA Reference Book, IENRI, Report, Oct. 2007.

[19] A.V. Durov, Y.V. Naidich and B.D. Kostyuk, J. Mater. Sci., 40 (2005) 2173–2178.

[20] W. Wang, C. Li, J. Li, J. Fan and X. Zhou, J. Rare Earth., 31(3) (2013) 289–295.

[21] G. Huang, L. Liu, L. Zhang and Z. Jin, J. Min. Metall. Sect. B-Metall., 52(2) (2016) 177-183.

[22] T.B. Reed, Free Energy Formation of Binary Compounds, MIT Press, Cambridge, MA, (1971).

[23] N. Mattern, J.H. Han, M. Zinkevich, O. Shuleshova, I. Kaban, D. Holland-Moritz, J. Gegner, F. Yang, J. Bednarčík, W. Löser and J. Eckert, Calphad, 39 (2012) 27–32.

[24] C. Wong, M. Zinkevich and F. Aldinger, Calphad, 28 (2004) 281–292.

[25] O. Fabrichnaya, Ch. Wang, M. Zinkevich, C. G. Levi, and F. Aldinger,. Phase Equilib. Diff., 26(6) (2005) 591–604.

[26] J.W. McMurray, Thermodynamic Modeling of Uranium and Oxygen Containing Ternary Systems with Gadolinium, Lanthanum, and Thorium, PhD Thesis, University of Tennessee, http://trace.tennessee.edu/utk_graddiss/3152, (2014). Accessed 18 May 2017.

[27] I. Barin, O. Knacke, Thermochemical properties of inorganic substances, Springer-Verlag Berlin Heidelberg New York, Verlag Stahleisen m.b.H. Dusseldorf, (1973) pp. 277-888.

[28] A. Passerone, M.L. Muolo, F. Valenza, F. Monteverde and N. Sobczak, Acta Mater., 57, (2009) 356–364.

[29] M.L. Muolo, F. Valenza, N. Sobczak, and A. Passerone, Adv. Sci. Technol., 64 (2011) 98–107.

[30] N. Sobczak, R. Nowak, A. Siewiorek, B. Korpala, G. Bruzda, I. Kaban, O. Shuleshova, J.H. Han, N. Mattern and J. Eckert, High temperature study of monotectic transformation, wetting and reactivity of liquid Gd-Ti alloys, Proc. of the 71st World Foundry Congress, Bilbao, Spain, (2014).

[31] L. Xi, I. Kaban, R. Nowak, G. Bruzda, N. Sobczak and J. Eckert, Wetting, reactivity and phase formation at the liquid Ni-Al/TiB_2 ceramic interfaces - be published in J. Am. Ceram. Soc.

[32] L. Fan, Y. Xie and X. Shu, Adv. Mat. Res., (1061-1062) (2015) 87-90.

[33] N. Eustathopoulos, Curr. Opin. Solid State Mater. Sci., 9(4) (2005) 152–160.